J. Fluid Mech. (2013), *vol.* 732, *pp.* 304–315.
doi:10.1017/jfm.2013.408

On the heat transferred to the air surrounding a semi-infinite inclined hot plate

Michael J. Gollner[1,†], Antonio L. Sánchez[2,3] and Forman A. Williams[2]

[1]Department of Fire Protection Engineering, University of Maryland, College Park, 3106 J.M. Patterson Building, College Park, MD 20742-3031, USA

[2]Department of Mechanical and Aerospace Engineering, University of California, San Diego, 9500 Gilman Dr., La Jolla, CA 92093-0411, USA

[3]Department of Thermal and Fluids Engineering, Universidad Carlos III de Madrid, Leganés, 28911, Spain

(Received 28 January 2013; revised 31 May 2013; accepted 2 August 2013)

An asymptotic analysis of laminar free convection in a boundary layer over an isothermal semi-infinite flat plate inclined at some angle to the vertical has been performed. Existing analytical solutions show no difference in the heat-transfer rate between the upper and lower surfaces of the plate, contrary to observations. To investigate this, higher-order perturbations of the non-dimensional temperature, velocity and pressure across the boundary layer were computed and found to show only small variations from first-order perturbations previously reported. Unexpectedly, third-order perturbations of all functions were found to be identical to those of the vertical plate, indicating that differences in temperature between both sides of the plate are limited to exceedingly small terms of order $x^{-9/4}$ or smaller, x being the distance from the leading edge, non-dimensionalized by the buoyancy length scale. Dominant differences between heat-transfer rates on the upper and lower surfaces were therefore concluded to be due to near-leading-edge effects. In applying an integral form of the conservation equations to the near-leading-edge region, it was found that, up to terms of order unity in x, the total heat-exchange rate for the inclined plate is identical to that of the vertical plate, so that the heat-transfer gain on one side balances exactly the loss occurring on the other. This simplification allowed determination of an upper bound for differences in heat-transfer rates between the upper and lower sides, even though complete determination of the differences would require a numerical integration of the full Navier–Stokes equations near the leading edge of the plate.

Key words: boundary layers, compressible boundary layers, compressible flows

1. Introduction

A recent study by Gollner *et al.* (2013) of flame spread over and under a plastic fuel at different angles of inclination revealed new flame-spread behaviour, where peak rates of flame spread were found on the underside of fuel surfaces, in contradiction with the traditional assumption that maximum spread rates occur in a vertical configuration. Because flame spread is governed by heat transfer from flames

† Email address for correspondence: mgollner@umd.edu

to unignited fuel, as described by Fernandez-Pello & Hirano (1978), a natural analogy can be drawn with heat transfer from an inclined, heated flat plate. This motivated the present analytical investigation of the simpler problem. Kierkus (1968) performed a first-order perturbation analysis of this problem for large Grashof numbers, but only in the Boussinesq approximation, finding no differences in the results between the upper and lower sides of the flat plate. Despite a later correction to Kierkus' work by Riley (1975), differences in the flow behaviour between the upper and lower surfaces of the inclined plate did not arise, in contrast to Kierkus' experimental observations.

In view of these experimental observations of differences between upper and lower surfaces and the lack of predictions of these differences by the expansions of Kierkus (1968), it is desirable to attempt to obtain an explanation. One possibility for this discrepancy is that expansions were not taken to high enough order, where differences could arise. Another possibility is that the differences arise from near-leading-edge effects that are not taken into account with such expansions. To investigate these possibilities, higher-order perturbation analyses and a study of near-leading-edge effects are performed here. Second-order and third-order perturbation analyses were performed, moreover taking into account density and viscosity variations associated with large temperature differences within the boundary layer. Contrary to expectations, the results indicate that differences between heat-transfer rates on the upper and lower surfaces do not appear in the laminar boundary-layer solution at these orders. On the other hand, it is shown that such differences can be evaluated by paying attention to near-leading-edge effects, which are not present in the boundary-layer asymptotic expansions, following a previous analysis of Messiter & Liñán (1976) for the vertical plate. By applying integral conservation equations to a control volume that includes the leading edge, an upper limit to the heat-transfer differences between the upper and lower surfaces is established. The analysis presented does not extend automatically to near-horizontal conditions, considered, for example, by Jones (1973), who showed theoretically that a small downward tilt of a heated upper surface leads to flow separation, without a singularity, through opposing pressure gradients of boundary-layer growth and buoyancy, and also, for example, by Gollner *et al.* (2013), who observed experimentally that even with a small upward tilt of a burning upward surface, boundary-layer flow separation also occurs.

2. Formulation

Consider the semi-infinite flat plate inclined at an angle ϕ to the vertical shown in figure 1. The plate temperature is a factor T_w larger than that of the surrounding atmosphere, where the heated air moves under the action of gravity. A straightforward order-of-magnitude analysis of the momentum balance equation reveals that the effects of molecular transport and buoyancy-induced convective flow are comparable in a non-slender Navier–Stokes region of characteristic size $[\mu_\infty'^2/(\rho_\infty'^2 g\cos\phi)]^{1/3}$ around the plate leading edge, where the velocity components are of order $(\mu_\infty' g\cos\phi/\rho_\infty')^{1/3}$, with g representing the gravitational acceleration and ρ_∞' and μ_∞' being the density and the viscosity of the ambient gas. With these characteristic scales used in defining dimensionless variables for the Navier–Stokes region, the problem is reduced to that of integrating

$$\frac{\partial}{\partial x}(\rho u)+\frac{\partial}{\partial y}(\rho v)=0 \tag{2.1}$$

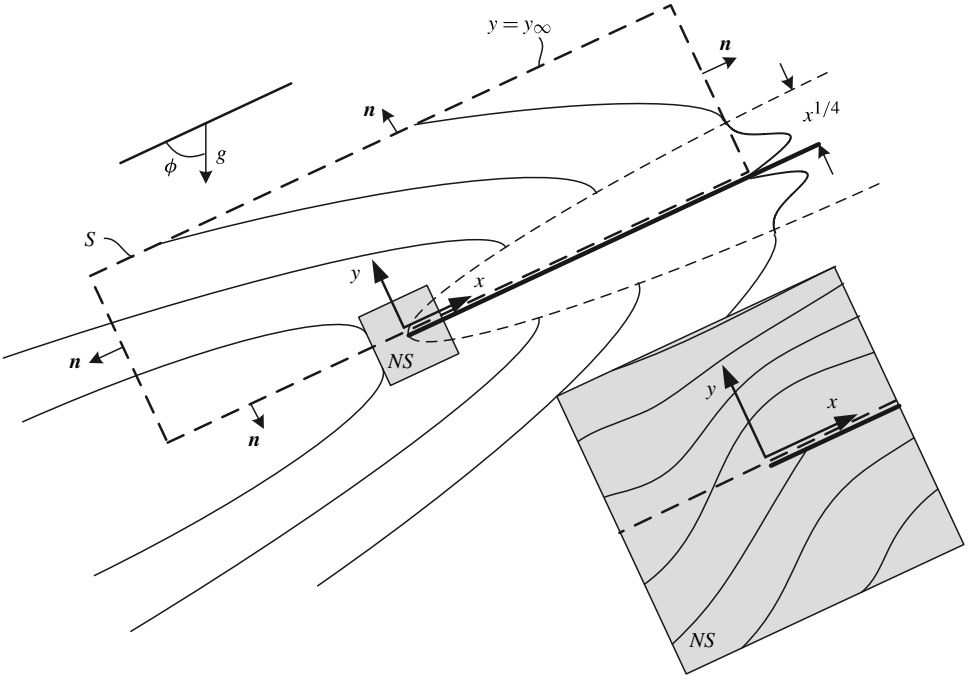

FIGURE 1. A schematic view of the flow around the inclined plate.

$$\rho u\frac{\partial u}{\partial x}+\rho v\frac{\partial u}{\partial y}=-\frac{\partial p}{\partial x}+1-\rho+\frac{\partial}{\partial x}\left[T^{\sigma}\left(\left(\frac{4}{3}+\mu_B\right)\frac{\partial u}{\partial x}-\left(\frac{2}{3}-\mu_B\right)\frac{\partial v}{\partial y}\right)\right]+\frac{\partial}{\partial y}\left[T^{\sigma}\left(\frac{\partial u}{\partial y}+\frac{\partial v}{\partial x}\right)\right] \tag{2.2}$$

$$\rho u\frac{\partial v}{\partial x}+\rho v\frac{\partial v}{\partial y}=-\frac{\partial p}{\partial y}+(1-\rho)\tan\phi+\frac{\partial}{\partial x}\left[T^{\sigma}\left(\frac{\partial u}{\partial y}+\frac{\partial v}{\partial x}\right)\right]+\frac{\partial}{\partial y}\left[T^{\sigma}\left(\left(\frac{4}{3}+\mu_B\right)\frac{\partial v}{\partial y}-\left(\frac{2}{3}-\mu_B\right)\frac{\partial u}{\partial x}\right)\right] \tag{2.3}$$

$$\rho u\frac{\partial T}{\partial x}+\rho v\frac{\partial T}{\partial y}=\frac{1}{Pr}\left[\frac{\partial}{\partial x}\left(T^{\sigma}\frac{\partial T}{\partial x}\right)+\frac{\partial}{\partial y}\left(T^{\sigma}\frac{\partial T}{\partial y}\right)\right] \tag{2.4}$$

with boundary conditions

$$\begin{cases} u=v=T-T_w=0 & \text{at } y=0 \text{ for } x>0 \\ u=v=T-1=p=0 & \text{as } (x^2+y^2)\to\infty \text{ for } y\neq 0,\, x>0. \end{cases} \tag{2.5}$$

Here, the coordinate x represents the distance measured along the plate from its tip, and y is the accompanying transverse coordinate, with u and v denoting the corresponding longitudinal and transverse velocity components. The variables T and ρ denote the temperature and density scaled with their ambient values, while p represents the pressure difference from the unperturbed ambient distribution, appropriately non-dimensionalized with its characteristic value $\rho_\infty'^{1/3}(\mu_\infty' g\cos\phi)^{2/3}$. These equations must be supplemented with the equation of state written in the

low-Mach-number approximation for an ideal gas as $\rho T = 1$. A power law with exponent σ has been assumed for the temperature dependence of all of the transport coefficients, with Pr and μ_B representing the constant values of the Prandtl number and of the ratio of bulk viscosity to shear viscosity for the ambient gas. According to (2.3) and (2.5), the solution depends on the plate-to-ambient temperature ratio T_w and on the inclination angle ϕ.

The characteristic size of the Navier–Stokes region is typically very small, giving for instance $[\mu_\infty'^2/(\rho_\infty'^2 g)]^{1/3} \simeq 0.293$ mm for the vertical plate in air at normal atmospheric conditions. Since in many practical applications the plates are considerably longer, there is interest in investigating the solution for the semi-infinite plate at large distances $x^2 + y^2 \gg 1$. The resulting flow field includes a boundary-layer region developing at distances $y \sim x^{1/4}$ from the plate surface surrounded by an outer inviscid region of slow motion driven by the boundary-layer entrainment. The problem can be conveniently described by introducing a stream function ψ, defined such that $\rho u = \partial\psi/\partial y$ and $\rho v = -\partial\psi/\partial x$. The outer flow is irrotational and isothermal to all orders, so that the equation for the corresponding stream function reduces to

$$\frac{\partial^2\psi}{\partial x^2} + \frac{\partial^2\psi}{\partial y^2} = 0, \tag{2.6}$$

which must be solved in terms of an expansion in inverse powers of the quadratic radial distance $x^2 + y^2$, leading to the form

$$\psi = (x^2 + y^2)^{3/8} f_2(\theta) + f_3(\theta) + (x^2 + y^2)^{-3/8} f_4(\theta) + \cdots, \tag{2.7}$$

with $\theta = \tan^{-1}(y/x)$ representing the polar angle. Appropriate boundary conditions for the different functions $f_i(\theta)$ at the plate surface, i.e. as $\theta \to 0$ and as $\theta \to 2\pi$, are obtained by matching with the boundary-layer flow, to be described in terms of the self-similar coordinate $\eta = |y|/x^{1/4}$ by introducing expansions of the form

$$\psi = x^{3/4} F_{1\pm}(\eta) + F_{2\pm}(\eta) + x^{-3/4} F_{3\pm}(\eta) + \cdots \tag{2.8a}$$

$$T = T_{1\pm}(\eta) + x^{-3/4} T_{2\pm}(\eta) + x^{-3/2} T_{3\pm}(\eta) + \cdots \tag{2.8b}$$

$$p = x^{1/4} P_{2\pm}(\eta) + x^{-1/2} P_{3\pm}(\eta) + \cdots. \tag{2.8c}$$

Different functions in principle must be considered on the upper and lower surfaces, as denoted in the formulation by the subscripts $+$ and $-$; in the development below, these additional subscripts are removed when referring to the self-similar functions for the vertical plate, the case treated by Clarke (1973).

Before proceeding with the analysis, it is worth mentioning that, as shown by Clarke (1973) for the vertical plate, the gas-flow problem in the boundary layer can be formulated alternatively in terms of a density-weighted coordinate through the so-called Howarth–Dorodnitsyn transformation. When the additional assumption $\sigma = 1$ is introduced, this transformation simplifies the vertical-plate problem considerably, in that at the first two orders the resulting boundary-layer description is identical to that for a Boussinesq fluid, independent of T_w. It can be seen, however, that for the inclined plate this coordinate transformation is somewhat less successful, in that the dependence on T_w, which is eliminated at leading order, remains however in the first-order corrections. Owing to this limitation, the use of the Howarth–Dorodnitsyn transformation offers only limited advantage for describing the corrections to the gaseous flow over an inclined plate and is therefore not adopted in the development below, which uses instead the variable $\eta = |y|/x^{1/4}$ along with a non-unity exponent $\sigma = 0.7$ for the temperature dependence of the transport coefficients, as corresponds

to air at moderately large temperatures. Thus, the development given in the following section extends the previous inclined-plate results of Kierkus (1968) and Riley (1975), limited to Boussinesq flow, to gaseous flow with $\sigma = 0.7$. Higher-order perturbations associated with the last terms shown in the expansions (2.8), not considered in previous flat-plate analyses, are also to be discussed below.

3. Results of the asymptotic development

The functions $F_{1\pm} = F_1$ and $T_{1\pm} = T_1$ can be determined by integrating the leading-order forms of (2.2) and (2.4)

$$[T_1^{\sigma}(T_1F_1')']' + \tfrac{3}{4}F_1(T_1F_1')' - \tfrac{1}{2}T_1(F_1')^2 + 1 - T_1^{-1} = 0 \tag{3.1}$$

$$[T_1^{\sigma}T_1']' + \tfrac{3}{4}PrF_1T_1' = 0 \tag{3.2}$$

with boundary conditions

$$F_1(0) = F_1'(0) = F_1'(\infty) = T_1(0) - T_w = T_1(\infty) - 1 = 0, \tag{3.3}$$

giving solutions on the upper and lower surfaces identical to those for the vertical plate. Here, the prime is used to denote differentiation with respect to the self-similar coordinate η. Sample profiles of temperature T_1 and velocity F_1' are shown in figure 2 for $Pr = 0.7$ and $\sigma = 0.7$. For a given wall temperature T_w the solution provides the value of the wall temperature gradient $T_1'(0)$ and of the entrainment velocity $F_1(\infty)$, giving for instance $T_1'(0) = (-0.1147, -0.2225, -0.3828)$ and $F_1(\infty) = (1.4656, 1.7083, 2.0353)$ for $T_w = (1.5, 2, 3)$. As shown by Kierkus (1968), the entrainment value enters when matching with the outer stream function to give $f_2(0) = F_1(\infty)$ and $f_2(2\pi) = -F_1(\infty)$ as boundary conditions for the first term in the expansion (2.7) of the outer stream function. As indicated by Riley (1975) for the inclined plate, this yields

$$f_2 = \sqrt{2}F_1(\infty)\sin\left[\frac{3}{4}\tan^{-1}\left(\frac{y}{x}\right) + \frac{\pi}{4}\right] \tag{3.4}$$

upon integration of the corresponding reduced Laplace equation, a result originally due to Clarke (1973) for the vertical plate.

The associated leading-order stream function $\psi_2 = (x^2 + y^2)^{3/8}f_2$ gives a non-zero slip velocity at the plate surface,

$$\left.\frac{\partial\psi_2}{\partial y}\right|_{y=0} = \frac{3}{4}x^{-1/4}F_1(\infty) \quad \text{for } x > 0, \tag{3.5}$$

that must be matched by the first-order correction to the velocity in the boundary layer. To determine the corresponding boundary-layer solution, computed by Riley (1975) for a Boussinesq fluid, one needs to compute the leading-order representation for the pressure variation across the boundary layer, determined by integrating the hydrostatic balance equation $P_{2\pm}' = \pm(1 - T_1^{-1})\tan\phi$ with boundary condition $P_{2\pm}(\infty) = 0$. The solution can be expressed conveniently in the form

$$P_{2\pm} = \pm\tan(\phi)\,\mathscr{P}_2 \tag{3.6}$$

in terms of the function

$$\mathscr{P}_2 = -\int_{\eta}^{\infty}(1 - T_1^{-1})\,\mathrm{d}\eta. \tag{3.7}$$

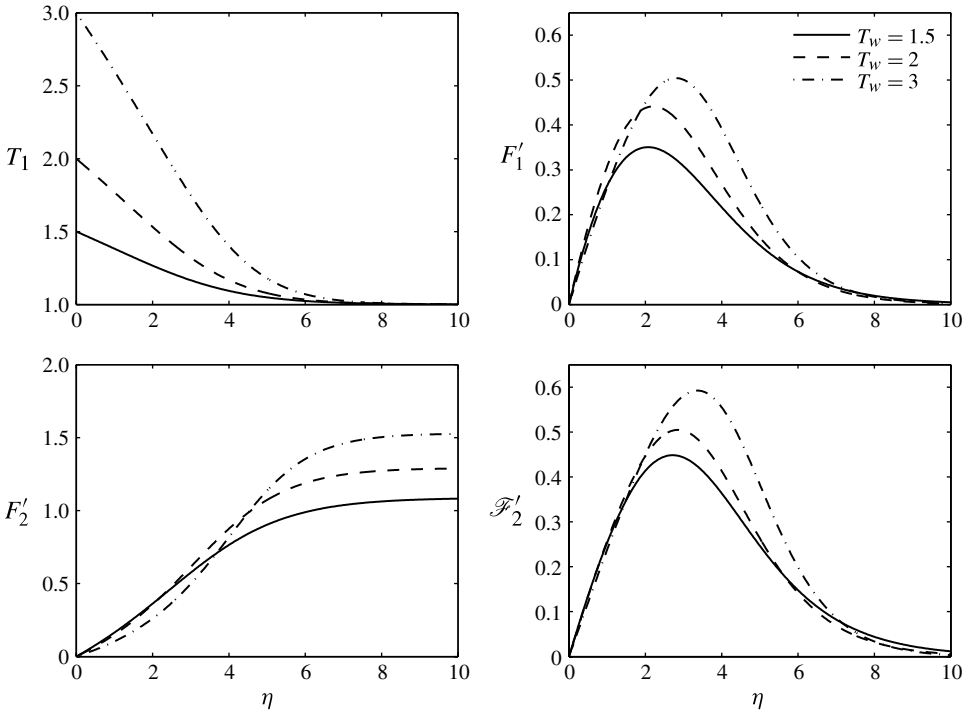

FIGURE 2. Boundary-layer solution for $Pr = 0.7$ and $\sigma = 0.7$ with $T_w = 1.5$ (solid curves), $T_w = 2$ (dashed curves) and $T_w = 3$ (dot-dashed curves); the upper plots show the leading-order temperature and velocity profiles T_1 and F_1' obtained from integration of (3.1) and (3.2) with boundary conditions (3.3), whereas the lower plots show the functions F_2' and $\mathscr{F}_2'$ for the first-order correction to the velocity, as obtained from integration of (3.10) and (3.11).

The solutions for $F_{2\pm}$ and $T_{2\pm}$ are determined by linear equations, obtained by collecting terms of order $x^{-3/4}$ and $x^{-5/4}$ in (2.2) and (2.4), respectively. In particular, convective terms involving derivatives of T_1 are seen to vanish at this order in (2.4), so that $T_{2\pm}$ is determined on both sides of the plate from the homogeneous problem

$$(T_1^{\sigma} T_{2\pm})'' + \tfrac{3}{4} Pr (F_1 T_{2\pm})' = 0, \quad T_{2\pm}(0) = T_{2\pm}(\infty) = 0 \tag{3.8}$$

whose solution is simply $T_{2\pm} = 0$, indicating that corrections to the local temperature field enter only at higher order, a result found previously for a Boussinesq fluid by Kierkus (1968) and Riley (1975) and also for gaseous flow with $\sigma = 1$ over a vertical plate Clarke (1973). Using this result in (2.2) yields

$$\left.\begin{aligned} &[T_1^{\sigma}(T_1 F_{2\pm}')']' + \tfrac{3}{4} F_1 (T_1 F_{2\pm}')' - \tfrac{1}{4} T_1 F_1' F_{2\pm}' = \pm \tfrac{1}{4} (\mathscr{P}_2 - \eta \mathscr{P}_2') \tan\phi \\ &F_{2\pm}(0) = F_{2\pm}'(0) = 0, \quad F_{2\pm}'(\infty) = \tfrac{3}{4} F_1(\infty) \end{aligned}\right\} \tag{3.9}$$

for the first-order correction for the stream function on the upper and lower surfaces F_{2+} and F_{2-}.

Owing to the linearity of (3.9), in expressing the dependence of $F_{2\pm}$ on the inclination angle ϕ it is convenient to refer the solution to that of the vertical plate, F_2,

obtained from

$$\left.\begin{array}{l}[T_1^{\sigma}(T_1F_2')']' + \frac{3}{4}F_1(T_1F_2')' - \frac{1}{4}T_1F_1'F_2' = 0,\\ F_2(0) = F_2'(0) = 0, \quad F_2'(\infty) = \frac{3}{4}F_1(\infty)\end{array}\right\}. \tag{3.10}$$

Subtracting (3.10) from (3.9) and dividing by $\tan\phi$ yields

$$\left.\begin{array}{l}[T_1^{\sigma}(T_1\mathscr{F}_2')']' + \frac{3}{4}F_1(T_1\mathscr{F}_2')' - \frac{1}{4}T_1F_1'\mathscr{F}_2' = \frac{1}{4}(\mathscr{P}_2 - \eta\,\mathscr{P}_2'),\\ \mathscr{F}_2(0) = \mathscr{F}_2'(0) = 0, \quad \mathscr{F}_2'(\infty) = 0\end{array}\right\} \tag{3.11}$$

for the function $\mathscr{F}_2 = \pm(F_{2\pm} - F_2)/\tan\phi$, thereby reducing the solution on the upper and lower plate surfaces to

$$F_{2\pm} = F_2 \pm \tan(\phi)\mathscr{F}_2. \tag{3.12}$$

Profiles of F_2' and $\mathscr{F}_2'$ are shown in figure 2 along with the leading-order results.

As $\eta \to \infty$ the solution of (3.10) and (3.11) yield, respectively, $F_2 - 3F_1(\infty)\eta/4 \to B$ and $\mathscr{F}_2 \to \mathscr{C}_2$, with $B = (-3.7094, -3.909, -5.7677)$ and $\mathscr{C}_2 = (2.0603, 2.1701, 2.5466)$ for $T_w = (1.5, 2, 3)$. According to (3.12), the corresponding asymptotic behaviours $F_{2\pm}(\eta \to \infty) = 3F_1(\infty)\eta/4 + C_{2\pm}$ involve the constants

$$C_{2\pm} = B \pm \tan(\phi)\mathscr{C}_2. \tag{3.13}$$

As shown in Riley (1975) for the case of a Boussinesq fluid, these constants appear in the boundary condition for the first-order correction to the outer stream function, obtained from integrating the reduced Laplace problem

$$\frac{\mathrm{d}^2 f_3}{\mathrm{d}\theta^2} = 0, \quad f_3(0) - C_{2+} = f_3(2\pi) + C_{2-} = 0 \tag{3.14}$$

to give

$$f_3 = C_{2+} - \frac{C_2}{\pi}\tan^{-1}\left(\frac{y}{x}\right) \tag{3.15}$$

when the polar coordinate is written in the form $\theta = \tan^{-1}(y/x)$. As noticed by Riley (1975), this last expression indicates that the symmetry of the streamline pattern for the inviscid outer flow is preserved at second order.

The analysis can be carried to the following order to determine in particular the functions $T_{3\pm}$, which introduce small corrections of order $x^{-3/2}$ to the leading-order result $T = T_1$, otherwise free from corrections up to this order because $T_{2\pm} = 0$. As an unexpected outcome, all functions $P_{3\pm}$, $F_{3\pm}$ and $T_{3\pm}$ are found to be identical to those of the vertical plate, i.e. $P_{3\pm} = P_3$, $F_{3\pm} = F_3$ and $T_{3\pm} = T_3$, with the latter result indicating that differences in temperature between both sides of the plate are limited to exceedingly small terms, of order $x^{-9/4}$ or smaller.

The way to see this result is to observe first that the higher-order analysis must begin by considering the pressure perturbation $P_{3\pm}$ across the boundary layer, which must match the pressure induced by the outer motion as dictated by $P_{3\pm} = -9F_1^2(\infty)/16$ as $\eta \to \infty$, obtained with use made of Bernoulli's equation $p + (u^2 + v^2)/2 = 0$ together with the leading-order stream function $\psi_2 = (x^2 + y^2)^{3/8} f_2$. Since $T_{2\pm} = 0$, the pressure changes at this order can be seen to be exclusively related to the leading-order fluid motion, with no hydrostatic effects, so that the resulting transverse momentum equation involves only the functions F_1 and T_1 but not the term proportional to $\tan\phi$, giving a pressure correction $P_{3\pm} = P_3$ equal to that of the vertical plate.

The analysis continues by using (3.15) to determine the apparent slip velocity

$$\left.\frac{\partial f_3}{\partial y}\right|_{y=0} = -\frac{C_2}{\pi x} \quad \text{for } x > 0, \tag{3.16}$$

needed to write the boundary condition

$$F'_{3\pm} - \tfrac{3}{8}F_1(\infty)\eta \to -C_2/\pi \tag{3.17}$$

for the velocity correction as $\eta \to \infty$ on both sides of the plate, independent of ϕ. Since the remaining boundary conditions, given by $F_{3\pm} = F'_{3\pm} = T_{3\pm} = 0$ at $\eta = 0$ and by $T_{3\pm} \to 0$ as $\eta \to \infty$, are also equal on both sides of the plate, and since the two sets of equations for the functions F_{3+} and T_{3+} and F_{3-} and T_{3-} are also identical, because terms involving $F_{2\pm}$, $P_{2\pm}$ or their derivatives are found to be absent, one can conclude that the functions $F_{3\pm} = F_3$ and $T_{3\pm} = T_3$ are simply those corresponding to the vertical plate irrespective of the inclination angle. Although differences may finally arise at order $x^{-9/4}$, their effects are unlikely to be of interest because of larger influences of the flow in the upstream Navier–Stokes region, addressed below.

4. Heat transfer from the plate

The temperature field obtained by numerical integration of the full problems (2.1)–(2.5) can be used in particular to determine the rate of heat transferred from the upper and lower surfaces of the plate, to be measured through the Nusselt numbers

$$Nu_\pm(x) = \mp\frac{1}{T_w - 1}\int_0^x \left(\frac{\partial T}{\partial y}\right)_{y=0\pm} \mathrm{d}x, \tag{4.1}$$

which have been scaled with the product of the gas conductivity at the wall temperature times the wall-to-ambient temperature difference. By making use of the boundary-layer temperature expansion (2.8), valid for $x \gg 1$, the Nusselt number can be expressed in the form

$$Nu_\pm(x) = -\frac{1}{T_w - 1}\left[\frac{4}{3}T'_{1\pm}(0)x^{3/4} + T'_{2\pm}(0)\ln(x) - \frac{4}{3}T'_{3\pm}(0)x^{-3/4} + O(x^{-3/2})\right], \tag{4.2}$$

which further reduces to

$$Nu_\pm(x) = -\frac{1}{T_w - 1}\left[\frac{4}{3}T'_1(0)x^{3/4} - \frac{4}{3}T'_3(0)x^{-3/4} + O(x^{-3/2})\right] \tag{4.3}$$

by observing that on both sides of the plate the first-order temperature corrections $T_{2\pm}$ are strictly zero, and the functions $T_{1\pm} = T_1$ and $T_{3\pm} = T_3$ are equal to those of the vertical plate.

This last result seems to indicate that differences in heat-transfer rates between the upper and lower surfaces of the plate would be only of order $x^{-3/2}$, their computation requiring consideration of small temperature corrections of order $x^{-9/4}$ involving the functions $T_{4\pm}(\eta)$. However, as noted by Messiter & Liñán (1976), the differences are actually larger, because the exact Nusselt number (4.1) includes an additional contribution of order unity, not present in (4.2), resulting from the heat transfer in the Navier–Stokes region, corresponding to distances $x \sim O(1)$. Since the flow is asymmetric in this region, because of the presence of the buoyancy force in (2.3), heat-transfer differences of order unity are expected to appear between the two sides of the plate.

The evaluation of this order-unity contribution to the Nusselt number requires, in principle, computation of the Navier–Stokes region. For the vertical plate, Messiter & Liñán (1976) showed how the order-unity correction may be computed by evaluating the integral form of the energy equation in a conveniently defined control volume, yielding a computation scheme that effectively links the correction to the Nusselt number to the results of the boundary-layer analysis. Their method is analogous to that used by Imai (1957) for computing the leading-edge contribution to the drag coefficient for a flat plate. We shall show below that the same procedure applied to the inclined plate, although failing to give the exact correction because of the asymmetry of the Navier–Stokes region in the present problem, in contrast to the symmetry of the previous Imai (1957) and Messiter & Liñán (1976) problems, nevertheless provides an upper bound to the heat-transfer difference, of interest in practical applications.

The development begins by using (2.1) to write (2.4) in the conservative form

$$\boldsymbol{\nabla}\cdot\left[\rho(T-1)\mathbf{v}-\frac{1}{Pr}T^{\sigma}\boldsymbol{\nabla}T\right]=0, \tag{4.4}$$

where $\mathbf{v}=(u,v)$ and $\boldsymbol{\nabla}=(\partial/\partial x,\partial/\partial y)$. By means of the divergence theorem, the integration of the above equation over a given control volume bounded by the closed surface S with unit normal vector $\boldsymbol{n}$ yields

$$\int_S \rho(T-1)\mathbf{v}\cdot\mathbf{n}\,\mathrm{d}S-\frac{1}{Pr}\int_S T^{\sigma}\boldsymbol{\nabla}T\cdot\mathbf{n}\,\mathrm{d}S=0, \tag{4.5}$$

stating that the outward flux of excess enthalpy must balance the conductive heating rate.

For the problem at hand, it is of interest to consider in the integration the rectangular control volume shown in figure 1, which includes sides parallel to the plate at $y=0$ and $y=y_\infty$ extending streamwise to distances from the leading edge much larger than unity. The control volume is closed by upstream and downstream boundaries perpendicular to the plate, with the downstream boundary located at a value of x, with $y_\infty \gg x^{1/4}\gg 1$, and the upstream face located away from the Navier–Stokes region. With the selection made, the top face $y=y_\infty$ and also the upstream face of the control volume lie in the inviscid isothermal region, where $T=1$, so that the integrands in (4.5) are identically zero. Similarly, at the downstream boundary non-negligible contributions appear only associated with the boundary-layer region corresponding to small distances $y\sim x^{1/4}$, because $T-1$ is exponentially small outside. The flux of excess enthalpy across the boundary layer

$$\int_S \rho(T-1)\mathbf{v}\cdot\mathbf{n}\,\mathrm{d}S=\int_0^{y\gg x^{1/4}}(T-1)\rho u\,\mathrm{d}y \tag{4.6}$$

can be written with use made of the boundary-layer results $T=T_1+O(x^{-3/2})$ and $\rho u=x^{1/2}F_1'+x^{-1/4}F_{2+}'$ to give

$$\int_0^{y\gg x^{1/4}}(T-1)\rho u\,\mathrm{d}y=x^{3/4}\int_0^{\infty}(T_1-1)F_1'\,\mathrm{d}\eta+\int_0^{\infty}(T_1-1)F_{2+}'\,\mathrm{d}\eta \tag{4.7}$$

up to terms of order unity. On the other hand, since the streamwise temperature gradient $\partial T/\partial x$ in the boundary layer is a small quantity of order x^{-1}, the associated

conductive heating rate, given by

$$-\frac{1}{Pr}\int_S T^\sigma \nabla T\cdot\mathbf{n}\,\mathrm{d}S=-\frac{1}{Pr}\int_0^{y\gg x^{1/4}} T^\sigma\frac{\partial T}{\partial x}\,\mathrm{d}y, \tag{4.8}$$

is of order $x^{-3/4}$, and consequently can be neglected if the analysis is restricted to terms of order unity or larger. As for the face $y=0$, the evaluation of (4.5) requires consideration of the plate surface for $x>0$, where the enthalpy flux is zero because $\mathbf{v}\cdot\mathbf{n}=0$, and also of the upstream stretch for $x<0$, to give in general

$$\int_S \rho(T-1)\mathbf{v}\cdot\mathbf{n}\,\mathrm{d}S-\frac{1}{Pr}\int_S T^\sigma\nabla T\cdot\mathbf{n}\,\mathrm{d}S=\frac{T_w^\sigma}{Pr}\int_0^x\left(\frac{\partial T}{\partial y}\right)_{y=0+}\mathrm{d}x$$
$$-\int_{-x}^0\left(\rho(T-1)v-\frac{T^\sigma}{Pr}\frac{\partial T}{\partial y}\right)_{y=0}\mathrm{d}x. \tag{4.9}$$

The last integral is identically zero for the vertical plate by the symmetry condition $v=\partial T/\partial y=0$ at $y=0$ for $x<0$. However, in the general case $\phi\neq 0$ we can expect this integral to give a non-zero contribution of order unity, because of the flow asymmetry in the Navier–Stokes region extending to distances of order $x\sim O(1)$ upstream from the plate edge.

Collecting now the different contributions of order unity or larger to the integral energy equation (4.5), given in (4.7) and (4.9), and using the result to solve for the Nusselt number Nu_+ defined in (4.1) we finally obtain

$$Nu_+=-\frac{4}{3}\frac{T_1'(0)}{T_w-1}x^{3/4}+\frac{Pr}{T_w^\sigma(T_w-1)}\int_0^\infty(T_1-1)F_{2+}'\,\mathrm{d}\eta$$
$$-\frac{Pr}{T_w^\sigma(T_w-1)}\int_{-x}^0\left(\rho(T-1)v-\frac{T^\sigma}{Pr}\frac{\partial T}{\partial y}\right)_{y=0}\mathrm{d}x \tag{4.10}$$

where integration by parts has been used together with (3.2) to write in (4.7)

$$\int_0^\infty(T_1-1)F_1'\,\mathrm{d}\eta=-\frac{4}{3Pr}T_w^\sigma T_1'(0). \tag{4.11}$$

Before discussing the result, one should note that the procedure presented above can be also applied in a mirror-symmetric control volume to give

$$Nu_-=-\frac{4}{3}\frac{T_1'(0)}{T_w-1}x^{3/4}+\frac{Pr}{T_w^\sigma(T_w-1)}\int_0^\infty(T_1-1)F_{2-}'\,\mathrm{d}\eta$$
$$+\frac{Pr}{T_w^\sigma(T_w-1)}\int_{-x}^0\left(\rho(T-1)v-\frac{T^\sigma}{Pr}\frac{\partial T}{\partial y}\right)_{y=0}\mathrm{d}x \tag{4.12}$$

for the corresponding Nusselt number on the lower side of the plate

As expected, equations (4.10) and (4.12) reproduce at leading order the boundary-layer result (4.3) and provide also the order-unity correction associated with the heat transfer near the tip of the plate through the integral terms in (4.10) and (4.12). While the integrals $\int_0^\infty(T_1-1)F_{2\pm}'\,\mathrm{d}\eta$ can be readily evaluated from the self-similar boundary-layer profiles, the last integral appearing in (4.10) and (4.12) requires in principle detailed knowledge of the temperature and velocity field along the plane $y=0$ in the non-slender viscous region just upstream from the plate, to be obtained from numerical integration of the Navier–Stokes problems (2.1)–(2.5). Detailed knowledge

of the Navier–Stokes region is however unnecessary for computing the total amount of heat transferred from the plate, as can be seen by adding (4.10) and (4.12) and using (3.12) to yield

$$Nu_+ + Nu_- = 2Nu, \tag{4.13}$$

where

$$Nu = -\frac{4}{3}\frac{T_1'(0)}{T_w - 1}x^{3/4} + \frac{Pr}{T_w^{\sigma}(T_w - 1)}\int_0^{\infty}(T_1 - 1)F_2'\,\mathrm{d}\eta, \tag{4.14}$$

is the two-term expansion for the Nusselt number corresponding to one side of the vertical plate, obtained in Messiter & Liñán (1976) for a Boussinesq fluid. Evaluation of the integral above gives $\int_0^{\infty}(T_1 - 1)F_2'\,\mathrm{d}\eta = (0.4238, 0.8149, 1.5484)$ for $T_w = (1.5, 2, 3)$.

According to (4.13), up to terms of order unity, the total heat exchange rate for the inclined plate is identical to that of the vertical plate, so that the heat transfer gain on one side balances exactly the loss occurring on the other according to

$$Nu_{\pm} - Nu = \pm\frac{Pr}{T_w^{\sigma}(T_w - 1)}\left[\tan(\phi)\int_0^{\infty}(T_1 - 1)\mathscr{F}_2'\,\mathrm{d}\eta - \int_{-x}^{0}\left(\rho(T-1)v - \frac{T^{\sigma}}{Pr}\frac{\partial T}{\partial y}\right)_{y=0}\mathrm{d}x\right], \tag{4.15}$$

obtained by subtracting (4.14) from (4.10) and (4.12). The first integral in the square brackets, $\int_0^{\infty}(T_1 - 1)\mathscr{F}_2'\,\mathrm{d}\eta$ is clearly positive, because both $(T_1 - 1)$ and $\mathscr{F}_2'$ are positive for $T_w > 1$, giving for instance $\int_0^{\infty}(T_1 - 1)\mathscr{F}_2'\,\mathrm{d}\eta = (0.3441, 0.7165, 1.6913)$ for $T_w = (1.5, 2, 3)$ with $Pr = 0.7$ and $\sigma = 0.7$. The second integral, representing the heat transferred by convection and conduction across the plane $y = 0$ for $x < 0$, provides an additional non-zero correction of order $\tan(\phi)$ when $\phi \neq 0$. In the presence of gravity, one expects the streamlines in the Navier–Stokes region to deflect upstream from the plate as indicated in the inset of figure 1, generating a transverse flow with $v > 0$ at $y = 0$, which in turn modifies the otherwise symmetric temperature field to give $\partial T/\partial y < 0$ along the plane $y = 0$. As a result, the local convective transport rate $\rho(T - 1)v$ and the heat conduction rate $-(T^{\sigma}/Pr)(\partial T/\partial y)$ across the plane are both expected to be positive. Consequently, the two integrals in (4.15) give contributions of different signs whose unknown difference determines the final sign of $Nu_{\pm} - Nu$. It is therefore not possible from this analysis to determine whether the inclination enhances or diminishes the resulting heat transfer on a given side of the plate. Nevertheless, the product of the first integral $\int_0^{\infty}(T_1 - 1)\mathscr{F}_2'\,\mathrm{d}\eta$ times $\tan(\phi)$ clearly provides an upper bound for the maximum possible heat-transfer gain (loss) on the upper (lower) plate surface. The heat-transfer rate on the upper surface therefore may exceed that on the lower surface at most by an amount determined by a Nusselt number of twice the magnitude of the first term in (4.15).

5. Conclusion

For the inclined plate, boundary-layer theory with up to third-order perturbations predicts that temperature differences are at most of the order of $x^{-9/4}$, much too small to explain the differences in the heat-transfer rate observed in both heat-transfer and fire experiments. Near-leading-edge effects may explain these observed differences. Although a simple analysis based on an integral conservation balance provides some

quantitative information, including upper bounds for differences in heat-transfer rates, full numerical integration of the upstream Navier–Stokes region will be needed in order to fully quantify leading-edge effects and thereby resolve the problem of different heat-transfer rates on the upper and lower surfaces of a heated, inclined semi-infinite flat plate.

Acknowledgements

The authors would like to thank D. Martinez Ruiz for his assistance in running numerical calculations and N. Riley and A. Liñán for pointing out their early contributions. Conversations with I. Jones on different aspects of the problem are also gratefully acknowledged.

REFERENCES

CLARKE, J. F. 1973 Transpiration and natural convection: the vertical-flat-plate problem. *J. Fluid Mech.* **57**, 45–61.

FERNANDEZ-PELLO, A. C. & HIRANO, T. 1978 Controlling mechanisms of flame spread. *Combust. Flame* **31**, 135–148.

GOLLNER, M. J., HUANG, X., COBIAN, J., RANGWALA, A. S. & WILLIAMS, F. A. 2013 Experimental study of upward flame spread of an inclined fuel surface. *Proc. Combust. Inst.* **34** (2), 2531–2538.

IMAI, I. 1957 Second approximation to the laminar boundary layer flow over a flat plate. *J. Aero. Sci.* **24**, 155–156.

JONES, D. R. 1973 Free convection from a semi-infinite flat plate inclined at a small angle to the horizontal. *Q. J. Mech. Appl. Math.* **26**, 77–98.

KIERKUS, W. T. 1968 An analysis of laminar free convection flow and heat transfer about an inclined isothermal plate. *Intl. J. Heat Mass Transfer* **11**, 241–253.

MESSITER, A. F. & LIÑÁN, A. 1976 The vertical plate in laminar free convection: effects of leading and trailing edges and discontinuous temperature. *J. Appl. Math. Phys. (ZAMP)* **27**, 633–651.

RILEY, N. 1975 Note on a paper by Kierkus. *Intl J. Heat Mass Transfer* **18**, 991–993.